

1. Introduction

Transmission density is an important physical property for exposed films in the fields of medicine, non-destructive testing, photography, and graphic arts. Standards for transmission density are provided by the National Institute of Standards and Technology (NIST) in the form of Standard Reference Materials (SRMs). These standards are film step tablets, 254 mm long by 35 mm wide, with steps extending the width of each film and equally spaced along its length. A double emulsion x-ray film is used for SRM 1001, while a single emulsion photographic film is used for SRM 1008. The steps have increasing transmission densities from approximately 0.1 to 4 from one end of the film to the other. SRM 1001 has 17 steps, while SRM 1008 has 23.

The transmission densities of film step tablets for both SRM 1001 and 1008 are determined with an instrument using the diffuse influx mode. Diffuse illumination is achieved with a flash opal, while directional detection is accomplished with a lens system. The transmitted radiant flux is detected by a temperature-controlled silicon (Si) photodiode with amplifier electronics capable of measuring signals spanning seven orders of magnitude. The instrument is designed to automatically measure many films using computerized data acquisition and control.

The organization of this Special Publication is as follows. The measurement equations relevant to the determination of transmission density using the diffuse influx mode are derived in section 2. The instrument used for measuring transmission density is described in section 3; its characterization, particularly in relation to the applicable international standards for this measurement, is detailed in section 4; and its operation is discussed in section 5. Finally, the uncertainties in the measured transmission density resulting from various components are derived in section 6.

2. Measurement Equations

The purpose of the measurement equations derived in this section is to obtain mathematical expressions of the transmission density as a function of different quantities. These quantities are the signals measured by the Si photodiode detector, the spectral properties of the influx and detected radiant flux, and the spatial properties of the radiant flux. Therefore, three measurement equations are derived and are used both for calculating transmission densities from experimental results and for determining the uncertainty in these transmission densities.

Two radiant fluxes are important for determining transmission density. Following the nomenclature given in [1, 2], these fluxes are the aperture flux Φ_i – the flux emerging from the sampling aperture in the directions and parts of the spectrum to be utilized in the measurement – and the transmitted flux Φ_t – the flux that passes through the specimen, emerging from a surface other than that on which the incident flux falls, and then utilized in the measurement. In terms of these fluxes, the transmittance factor T is given by

$$T = \frac{\Phi_{\tau}}{\Phi_j} \quad (2.1)$$

and the transmission density D_T is defined by

$$D_T = -\log_{10} T . \quad (2.2)$$

To this point, neither the geometrical nor spectral properties of the fluxes have been specified. For diffuse transmission density, either the incident flux (influx) must be diffuse or detection must include both the regular and diffuse components of the transmitted flux (efflux) [3]. Therefore, two equivalent experimental modes are possible for measuring diffuse transmission density: the diffuse influx mode, in which the illumination is diffuse and the detection is directional, and the diffuse efflux mode, in which the illumination is directional and the detection is diffuse.

Likewise, the spectral properties of the fluxes are defined for diffuse transmission density [4]. The relative spectral flux distribution of the incident flux is denoted by S_H and is based on the spectral flux distribution of the CIE Standard Illuminant A modified in the infrared region to protect the sample and optical elements from excessive heat. For visual transmission density, the combined spectral response of the detector and the spectral characteristics of the optical elements collecting the transmitted flux is denoted by V_T . The spectral product is obtained by multiplying, at each wavelength, the spectral power of the influx spectrum by the spectral response of the receiver. The spectral product is specified to be the same as the product of CIE Standard Illuminant A, S_A , with the spectral luminous efficiency function for photopic vision, V_{λ} . Therefore, at each wavelength,

$$S_H \cdot V_T = S_A \cdot V_{\lambda} . \quad (2.3)$$

In terms of the definitions and concepts presented in the previous paragraphs, the instrument measures diffuse visual transmission density using the diffuse influx mode. The important components of the instrument are shown in figure 2.1, as well as a spherical coordinate system. The film step tablet is in contact with the opal, which provides an influx with angles of incidence θ from 0° to 90° and a relative spectral flux distribution S_H . The efflux is collected within an acceptance cone having a half-angle κ less than 10° and with a spectral response V_T . Therefore, using the functional notation specified in [1, 2, 3], the measured transmission density is described by

$$D_T(90^\circ \text{ opal}; S_H; \leq 10^\circ; V_T) . \quad (2.4)$$

The properties of the various components used in deriving the measurement equations are given in table 2.1. The influx has radiance $L_j(\lambda)$, where λ is the wavelength. The opal has reflectance $\rho_o(\lambda)$ and diffusion coefficient d (defined below),

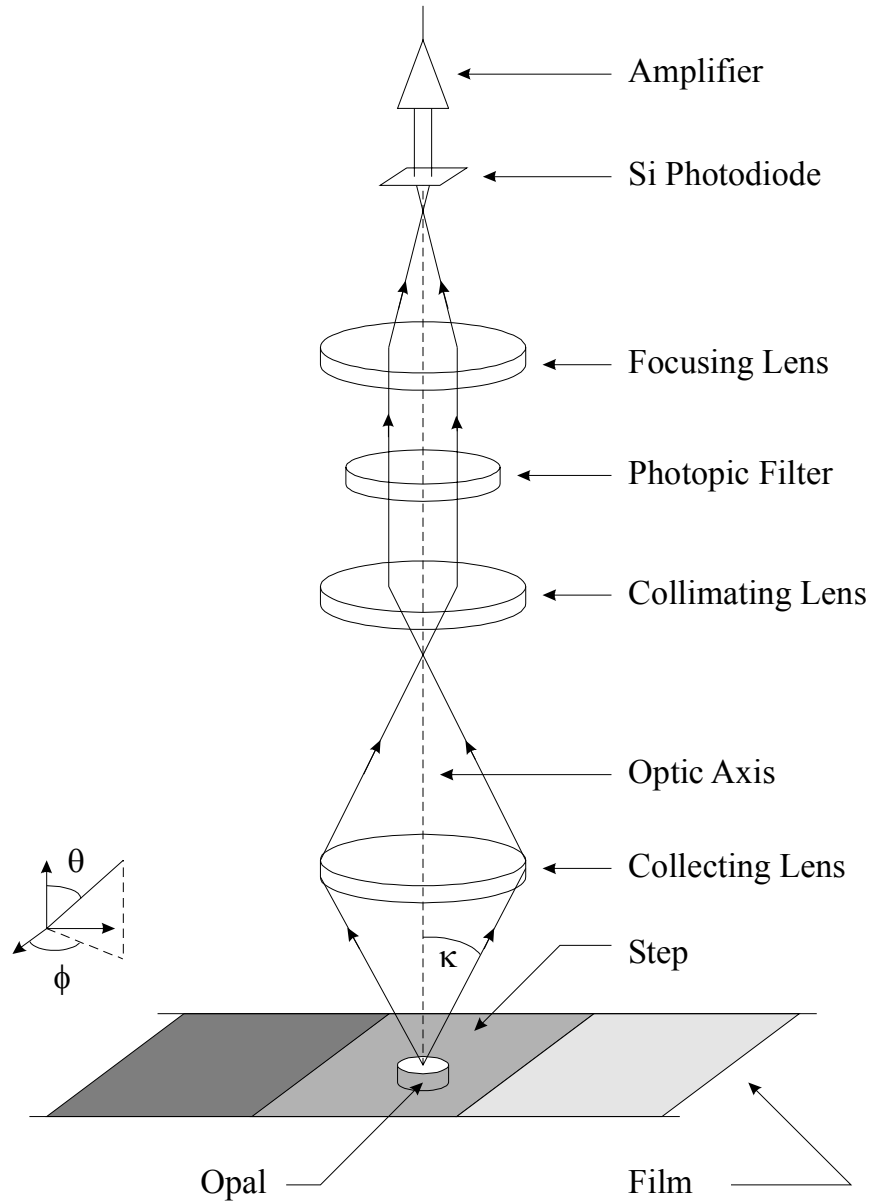


Figure 2.1 Important components of the diffuse transmittance densitometer.

while the step being measured has transmittance $\tau_s(\lambda)$ and reflectance $\rho_s(\lambda)$. The efflux has radiance $L_r(\lambda)$. As shown in section 3, the aperture stop of the optical system is the collection lens. Therefore, to first order, the throughput is given by $A \cdot \Omega$, where A is the area of the opal and Ω is the solid angle, with half-angle κ , from the center of the opal to the edges of the collection lens. Note that the opal is the aperture of the system defining the aperture flux Φ_j . The photopic filter has transmittance $\tau_f(\lambda)$, the photodiode has spectral responsivity $R(\lambda)$, and the amplifier has gain G .

Table 2.1 Properties and symbols of components of transmission density instrument

Property	Symbol
Influx radiance	$L_j(\lambda)$
Opal reflectance	$\rho_o(\lambda)$
Opal diffusion coefficient	d
Step transmittance	$\tau_s(\lambda)$
Step reflectance	$\rho_s(\lambda)$
Efflux radiance	$L_t(\lambda)$
Acceptance cone half-angle	κ
Filter transmittance	$\tau_f(\lambda)$
Photodiode responsivity	$R(\lambda)$
Amplifier gain	G

The differential radiant flux $d\Phi$ from the opal or the step to the collecting lens is given by

$$d\Phi(\lambda, a, \omega) = L(\lambda, a, \omega) \cdot da \cdot d\omega, \quad (2.5)$$

where a is a point on the opal or step and ω is a direction with angles θ and ϕ . Assume that the radiance $L(\lambda, a, \omega)$ is constant within the acceptance cone. Then, by integrating eq (2.5) over the spatial variables the spectral flux $\Phi(\lambda)$ is given by

$$\begin{aligned} \Phi(\lambda) &= \iint d\Phi(\lambda, a, \omega) \cdot da \cdot d\omega \\ &= L(\lambda) \cdot A \cdot \Omega, \end{aligned} \quad (2.6)$$

which is the spectral flux incident on the photopic filter. The photopic filter modifies this flux so that the spectral flux incident on the photodiode is given by

$$\Phi(\lambda) = L(\lambda) \cdot \tau_f(\lambda) \cdot A \cdot \Omega. \quad (2.7)$$

For the opal, the spectral radiance is

$$L(\lambda) = L_j(\lambda), \quad (2.8)$$

while for the step the spectral radiance is

$$\begin{aligned}
L(\lambda) &= L_\tau(\lambda) \\
&= L_j(\lambda) \cdot \frac{\tau_s(\lambda)}{1 - \rho_o(\lambda) \cdot \rho_s(\lambda)} ,
\end{aligned} \tag{2.9}$$

showing that the radiance from the opal is modified by the transmittance of the step and by inter-reflections between the opal and the step. Combining eq (2.7) with eqs (2.8) and (2.9) yields the spectral aperture and transmitted fluxes, respectively. Thus, the spectral aperture flux is

$$\Phi_j(\lambda) = L_j(\lambda, \omega) \cdot \tau_f(\lambda) \cdot A \cdot \Omega \tag{2.10}$$

and the spectral differential transmitted flux is

$$\Phi_\tau(\lambda) = L_j(\lambda, \omega) \cdot \frac{\tau_s(\lambda, \omega)}{1 - \rho_o(\lambda) \cdot \rho_s(\lambda)} \cdot \tau_f(\lambda) \cdot A \cdot \Omega . \tag{2.11}$$

The spectral output current $I(\lambda)$ from the photodiode, for either the spectral aperture flux or the spectral transmitted flux, is given by

$$I(\lambda) = \Phi(\lambda) \cdot R(\lambda) . \tag{2.12}$$

The total current I is obtained by integrating eq (2.12) over wavelength, yielding

$$\begin{aligned}
I &= \int dI(\lambda) \\
&= \int \Phi(\lambda) \cdot R(\lambda) \cdot d\lambda .
\end{aligned} \tag{2.13}$$

From eq (2.13) and eqs (2.10) and (2.11), the current from the aperture flux I_j is given by

$$I_j = A \cdot \Omega \cdot \int L_j(\lambda) \cdot \tau_f(\lambda) \cdot R(\lambda) \cdot d\lambda \tag{2.14}$$

and the current from the transmitted flux I_τ by

$$I_\tau = A \cdot \Omega \cdot \int L_j(\lambda) \cdot \frac{\tau_s(\lambda)}{1 - \rho_o(\lambda) \cdot \rho_s(\lambda)} \cdot \tau_f(\lambda) \cdot R(\lambda) \cdot d\lambda . \tag{2.15}$$

Note that the currents in eqs (2.14) and (2.15) are proportional to the radiant flux and contain both the spectral and geometrical information specified by eq (2.4). In terms of the nomenclature,

$$S_H \propto L_j(\lambda, \omega) \tag{2.16}$$

and

$$V_T = \tau_f(\lambda) \cdot R(\lambda) . \quad (2.17)$$

Finally, the measured signal S , a voltage, is given by

$$S_j = I_j \cdot G_j \quad (2.18)$$

for the aperture flux and by

$$S_\tau = I_\tau \cdot G_\tau \quad (2.19)$$

for the transmitted flux.

Reexpressing eq (2.2) in terms of the aperture and transmitted fluxes, the transmission density is

$$D_T = \log_{10} \left(\frac{\Phi_j}{\Phi_\tau} \right) . \quad (2.20)$$

The first two measurement equations derived below depend upon the currents being proportional to the fluxes, so that eq (2.20) is equivalent to

$$D_T = \log_{10} \left(\frac{I_j}{I_\tau} \right) . \quad (2.21)$$

For transmission density as a function of the measured signals, the first measurement equation is obtained by substituting eqs (2.18) and (2.19) into eq (2.21) to yield

$$D_T = \log_{10} \left(\frac{S_j \cdot G_\tau}{S_\tau \cdot G_j} \right) . \quad (2.22)$$

The second measurement equation expresses the transmission density as a function of the spectral variables. Using eq (2.14) and (2.15) and considering only the wavelength dependence of the variables, eq (2.21) becomes

$$D_T = \log_{10} \left(\frac{\int L_j(\lambda) \cdot \tau_f(\lambda) \cdot R(\lambda) \cdot d\lambda}{\int L_j(\lambda) \cdot \frac{\tau_s(\lambda)}{1 - \rho_o(\lambda) \cdot \rho_s(\lambda)} \cdot \tau_f(\lambda) \cdot R(\lambda) \cdot d\lambda} \right) . \quad (2.23)$$

The transmission density as a function of the spatial variables is given by the third measurement equation. The derivation which follows is adapted from [5]. Considering only the spatial variables, the radiant flux incident on the photodiode is a fraction of the total efflux. Integrating eq (2.5) over the spatial variables and ignoring the wavelength yields a flux of

$$\Phi = \iint L(a, \omega) \cdot da \cdot d\omega . \quad (2.24)$$

Assuming that the radiance $L(a, \omega)$ is constant over the area of the opal and over all azimuthal angles ϕ , eq (2.24) becomes

$$\Phi = 2\pi \cdot A \cdot \int L(\theta) \cdot \cos\theta \sin\theta \cdot d\theta . \quad (2.25)$$

For the measured aperture and transmitted fluxes Φ_j and Φ_τ , respectively, the limits of integration in eq (2.25) are 0 to κ , while for the total aperture and transmitted fluxes $\Phi_{T,j}$ and $\Phi_{T,\tau}$, respectively, the limits are 0 to $\pi/2$. The ratios of these fluxes are given by

$$\frac{\Phi_j}{\Phi_{T,j}} = \frac{\int_0^\kappa L_j(\theta) \cdot \cos\theta \sin\theta \cdot d\theta}{\int_0^{\pi/2} L_j(\theta) \cdot \cos\theta \sin\theta \cdot d\theta} \quad (2.26)$$

and

$$\frac{\Phi_\tau}{\Phi_{T,\tau}} = \frac{\int_0^\kappa L_\tau(\theta) \cdot \cos\theta \sin\theta \cdot d\theta}{\int_0^{\pi/2} L_\tau(\theta) \cdot \cos\theta \sin\theta \cdot d\theta} . \quad (2.27)$$

Substituting eqs (2.26) and (2.27) into the definition of transmission density given by eq (2.20) yields

$$D_T = \log_{10} \left(\frac{\Phi_{T,j} \cdot \frac{\int_0^\kappa L_j(\theta) \cdot \cos \theta \sin \theta \cdot d\theta}{\int_0^{\pi/2} L_j(\theta) \cdot \cos \theta \sin \theta \cdot d\theta}}{\Phi_{T,\tau} \cdot \frac{\int_0^\kappa L_\tau(\theta) \cdot \cos \theta \sin \theta \cdot d\theta}{\int_0^{\pi/2} L_\tau(\theta) \cdot \cos \theta \sin \theta \cdot d\theta}} \right). \quad (2.28)$$

Assuming that the opal is Lambertian for $0 \leq \theta \leq \kappa$, $L_j(\theta)$ is constant for these angles. Furthermore, assume that the scattering properties of the step make it Lambertian for $0 \leq \theta \leq \pi/2$. Therefore, eq (2.28) reduces to

$$D_T = \log_{10} \left(\frac{\Phi_{T,j} \cdot \int_0^{\pi/2} \cos \theta \sin \theta \cdot d\theta}{\Phi_{T,\tau} \cdot \int_0^{\pi/2} \frac{L_j(\theta)}{L_j(0)} \cdot \cos \theta \sin \theta \cdot d\theta} \right), \quad (2.29)$$

where $L_j(0)$ is the radiance from the opal at $\theta=0$. Defining the diffusion coefficient d to be

$$d = \frac{\int_0^{\pi/2} \frac{L_j(\theta)}{L_j(0)} \cdot \cos \theta \sin \theta \cdot d\theta}{\int_0^{\pi/2} \cos \theta \sin \theta \cdot d\theta}, \quad (2.30)$$

eq (2.29) becomes

$$D_T = \log_{10} \left(\frac{\Phi_{T,j}}{\Phi_{T,\tau}} \cdot \frac{1}{d} \right). \quad (2.31)$$

The three measurement equations are given by eqs (2.22), (2.23), and (2.31). The first is the method for calculating D_T from the measured signals and the gains, while the second relates D_T to the spectral properties of the influx, opal, step, photopic filter, and photodiode. The third measurement equation expresses the dependence of D_T on the

spatial properties of the aperture flux, accounting for the non-Lambertian quality of the opal.

3. Description of Instrument

The instrument was designed and built to automatically measure the diffuse visual transmission density of film step tablets using the diffuse influx mode. The major optical and electronic components are those shown in figure 2.1. A computer controls the entire measurement sequence. This section provides a detailed description of the instrument, which is conveniently divided into three systems: the source, the film transport, and the detector. A list of all the components of the instrument is given in table 3.1.[†]

The source system provides a diffuse illumination to the film step tablet with the correct spectral flux distribution. The system consists of a lamp and housing, an infrared filter assembly, a shutter, and an opal assembly. A cross section of the source system is shown in figure 3.1. Starting from the bottom of the figure, a 100 W quartz-tungsten-halogen lamp is contained in a lamp housing. The lamp is burned in at 8.0 A for 24 h and then at 7.8 A for an additional 48 h prior to being used for measurements. An elliptical reflector focuses the light from this lamp at approximately the position of the opal. The lamp housing is cooled with distilled water at a temperature of 25 °C pumped through a chiller, and a constant dc current is run through the lamp from a power supply. If the flow of water is interrupted, the flow meter closes a switch, which in turn disables the power supply. This prevents the infrared filter assembly, described next, from overheating.

The infrared filter assembly consists of aluminum plates for mounting to the lamp housing and the shutter and an infrared filter. Infrared filtering is accomplished with a combination of water and an optical filter. Distilled water is circulated, using the same chiller as for the lamp housing, through the stainless steel water filter in the direction indicated in figure 3.1. This water absorbs most of the light at infrared wavelengths, as well as cooling the plates which seal, with rubber gaskets, the top and bottom of the water filter. The bottom plate is simply a piece of BK-7 glass with a diameter of 100 mm and a thickness of 4 mm. The top plate is an optical filter, Hoya LP-15, with the same diameter and thickness as the glass plate. The optical filter was chosen so that its transmittance would modify the spectral flux distribution from the lamp to one approximating S_H . When the shutter is closed, it blocks all light from reaching the opal so that a background signal can be measured. A controller operates the shutter and is interfaced to the computer.

[†] Certain commercial equipment, instruments, or materials are identified in this paper to specify adequately the experimental procedure. Such identification does not imply recommendation or endorsement by the National Institute of Standards and Technology, nor does it imply that the materials or equipment identified are necessarily the best available for the purpose.

Table 3.1 Components of diffuse transmission densitometer

Component	Description	Manufacturer	Model
Lamp	100 W quartz-tungsten-halogen	Oriel	6333
Lamp Housing			
Shell		Oriel	60100
Reflector	Ellipsoidal, f/2	Oriel	60112
Lamp Power Supply	20 V, 10 A	Hewlett-Packard	6642A
Optical Filter	Infrared cut-off	Hoya	LP-15
Water Chiller		Lytron	MCS10G01
Flow Meter		Proteus	G203C24
Shutter		Vincent Assoc.	VS35
Shutter Controller		JML Optical Industries	SDS 16555
Motion Controller		Aerotech	DR 500 with three DS 16020
Horizontal Stage		Aerotech	ATS70090-U-TB
Vertical Stage		Aerotech	ATS02010-U-40L
Solenoid Valve		Atkomatic	S240-4-V-N
Electro-mechanical Relay		National Instruments	ER-16
Collecting Lens	Biconvex, BK-7, 75.6 mm focal length	Newport	KBX048AR.14
Collimating Lens, Focusing Lens	Biconvex, BK-7, 38.1 mm focal length	Newport	KBX139AR.14
Photopic Filter		Graseby	
Photodiode	Si	Hamamatsu	1227-1010BQ
Photodiode Amplifier		Reyer Corp.	S10/3 - RC
Temperature Controller		ILX	LDT-5412
Digital Voltmeter		Hewlett-Packard	3457A

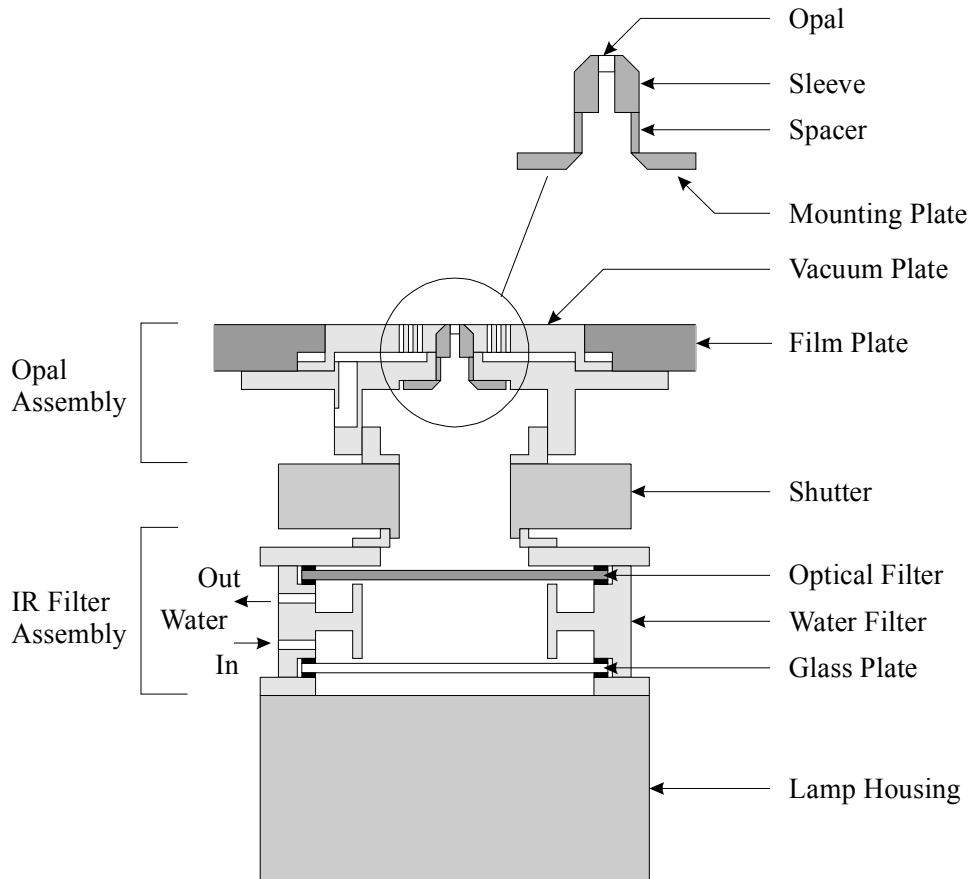


Figure 3.1 Cross-section of the source system for providing a diffuse influx.

The opal assembly consists of a plate for mounting to the shutter, two large pieces — one for holding the opal and mounting to the film plate and the other to provide a vacuum for bringing the film step tablet in contact with the opal (described below) — and several smaller pieces for mounting the opal. All the pieces are aluminum, and the vacuum plate is black-anodized. A flash opal with a diameter of 3 mm and a thickness of 1.5 mm is the source of diffuse illumination. The opal is fit partially into the black-anodized sleeve and held in place with black tape. The depth of the opal in the sleeve and the height of the spacer are adjusted so that the top of the opal is aligned with the vacuum plate when the opal assembly is complete. Black enamel paint is used so that all the light incident on the film step tablet originates from the top of the opal, which defines the sampling aperture for the influx. This paint is applied to the sides of the opal and between the opal and the sleeve. The sleeve and spacer are inserted in the opal plate and a mounting plate attached to the opal plate holds the sleeve in place.

The film transport system picks up a film from a tray, positions the film to measure the transmission density of each step on the film, and drops the film in another tray. A top view of this system is shown in figure 3.2, while a cross section of the film holder and opal assembly is shown in figure 3.3. The film trays consist of flat aluminum

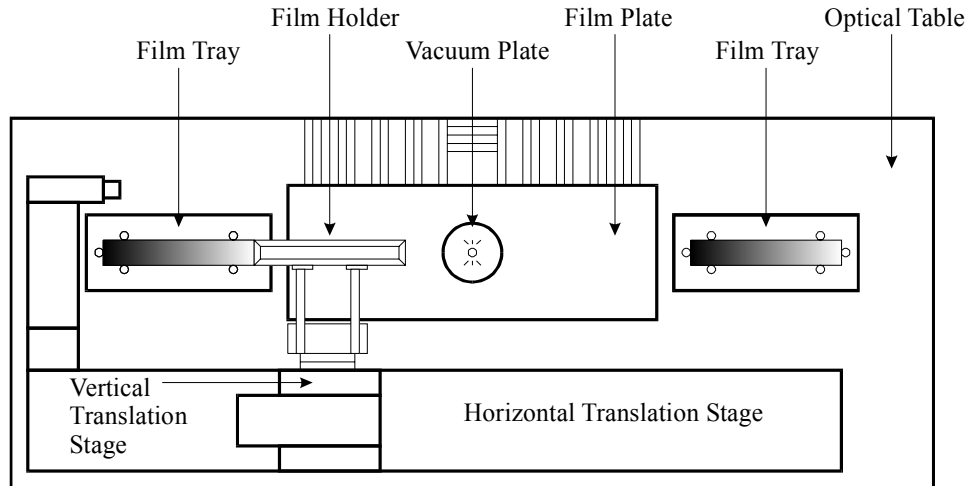


Figure 3.2 Top view of the film transport system.

plates with vertical posts to hold the films in the proper position. The film tray on the left side in figure 3.2 holds the films to be measured, while the one on the right side holds those that have been measured. The film holder, made of black-anodized aluminum, is attached to a vertical spring-loaded stage on a vertical translation stage, which in turn is attached to a horizontal translation stage. Both translation stages have absolute encoders. The film holder and translation stages move the films to the appropriate location; the sequence is described in section 5. The film plate is black-anodized aluminum and supports the part of the film that is not on the vacuum plate.

A vacuum both holds the film on the film holder and brings the film into direct contact with the opal. The vacuum is applied through solenoids controlled by the computer. The film holder has a groove along its outer edge, as shown in figure 3.3. When the film holder is in contact with a film and a vacuum is applied to this groove, the film is attached to the film holder and can be moved vertically and horizontally with the translation stages. There are small holes in the vacuum plate of the opal assembly, shown in cross-section in figure 3.3 and with a pattern indicated in figure 3.2. When a film is on the vacuum plate and a vacuum is applied between the opal and vacuum plates, the film is pulled down onto the opal.

The detector system collects the efflux within an acceptance cone and focuses this radiant flux onto the Si photodiode for detection. A cross section of this system is shown in figure 3.4, along with the marginal and chief rays. All the lenses have diameters of 5 cm and are made of BK-7 glass. The lenses perform the functions indicated by their designations: collecting the light within the acceptance cone, collimating it through the photopic filter, and focusing it onto the detector. A baffle with a diameter of 10 mm reduces scattered light in the detector system. The spectral transmittance of the photopic filter is such that, in combination with the spectral response of the Si photodiode, the spectral response of the detector system closely approximates the photopic spectral luminous efficiency function. The photopic filter is slightly tilted so that the light

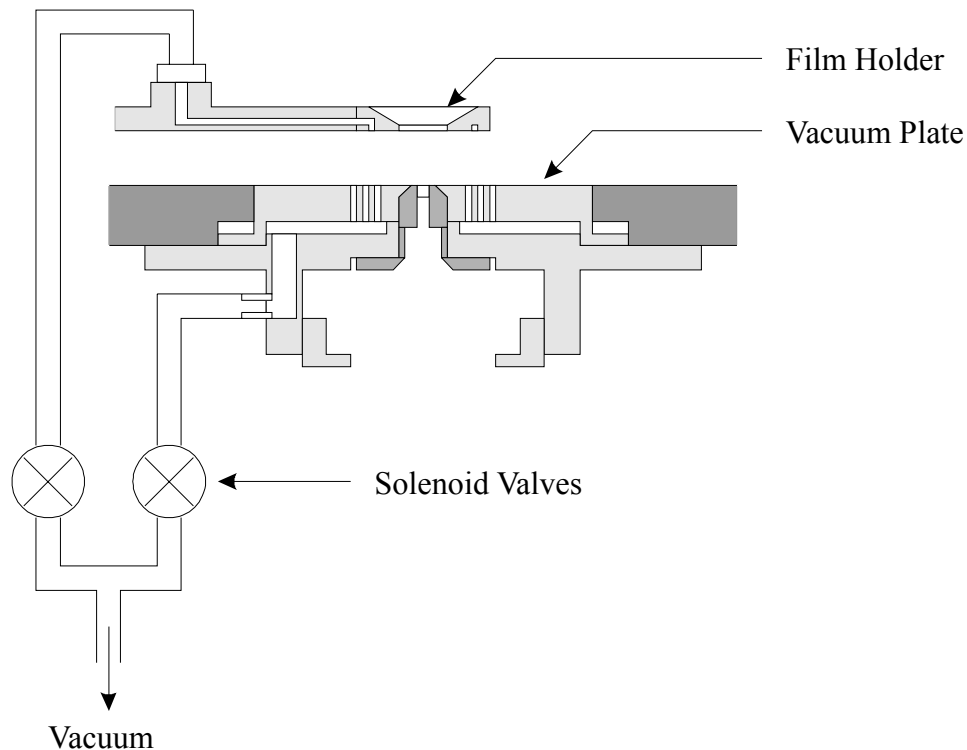


Figure 3.3 Cross-section of the film holder and opal assembly of the film transport system.

reflected from it does not travel back down to the opal. The lenses, baffle, and filter are housed in a black-anodized aluminum cylinder. The 4 mm by 4 mm Si photodiode is contained in a package that provides both thermoelectric temperature control at 25 °C and current-to-voltage conversion with a gain that can be selected either manually or automatically. Light reflected from the Si photodiode back onto the opal has no measurable effect on the values of visual transmission density.

The aperture stop of the optical system is the collecting lens, which defines an acceptance cone with a half-angle $\kappa = 9.5^\circ$ between it and the opal. If the opal is included in the optical system, it is the field stop. However, the step of a film diffuses the transmitted light, making the area from which light exits the film ill-defined. Therefore, if the opal is not included in the optical system, the photodiode is the field stop. The field of view has a diameter of 10 mm at the position of the opal, which is large enough to capture the entire area from which light exits the film.

The systems of the instrument described above – source, transport, and detection – are located on an optical table. The horizontal translation stage and film trays are attached directly to the table, as is a vertical post of 80/20 aluminum to which the lamp housing, film plate, and optic housing attach. The mounting plate of the source attaches to the film plate, as shown in figure 3.1, and the photodiode package attaches to the optic housing, as shown in figure 3.4. The solenoids that control the vacuum are also attached

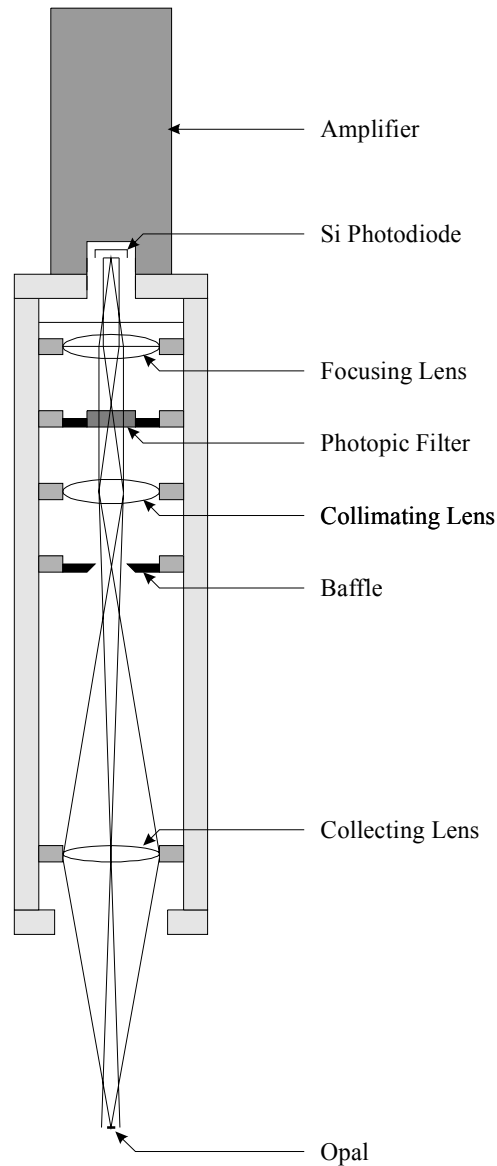


Figure 3.4 Cross-section of the detection system, including the marginal and chief

to the vertical post. The electronics used with the instrument are located in a rack adjacent to the optical table.

A schematic diagram showing all the components of the instrument and their connections is shown in figure 3.5. A computer performs all the data acquisition and control, using a program written in Visual Basic. The GPIB interface communicates with the lamp power supply and the digital voltmeter. Separate, custom cards control the electro-mechanical relays and the motion controller.

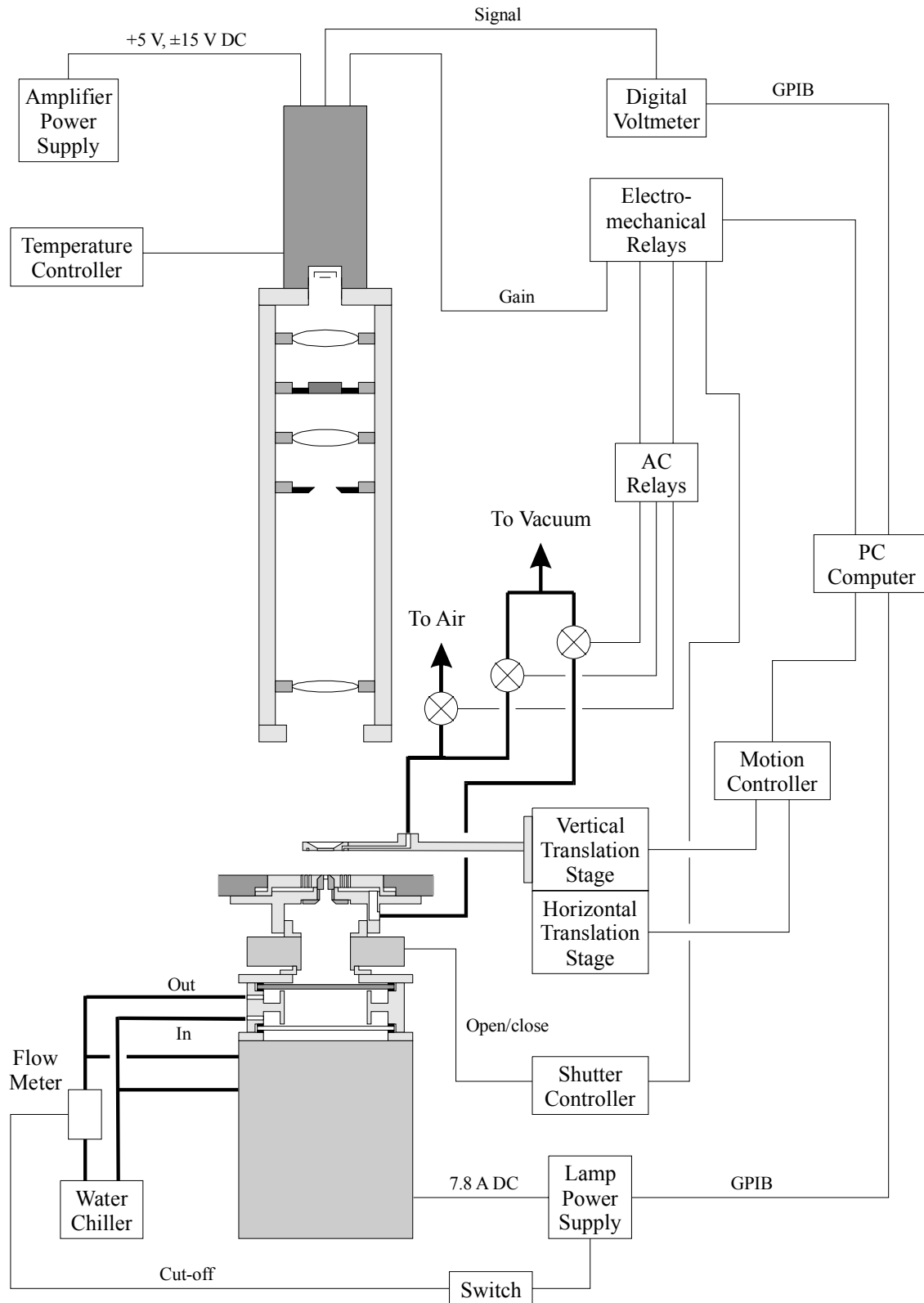


Figure 3.5 Schematic diagram of all the components of the diffuse transmittance densitometer and their connections

Most of the automatic experimental control is achieved with the electro-mechanical relays, which are powered from an external voltage supply. One relay provides signals to the shutter controller, which in turn opens or closes the shutter. The two solenoids on the vacuum lines are also opened and closed using ac relays controlled by signals from the electro-mechanical relays. The gain on the photodiode amplifier is set using the signals from three relays. The remainder of the automatic experimental control is achieved by the linear translation stages, which are operated by the motion controller. A diagram of the electrical connections is shown in figure 3.6.

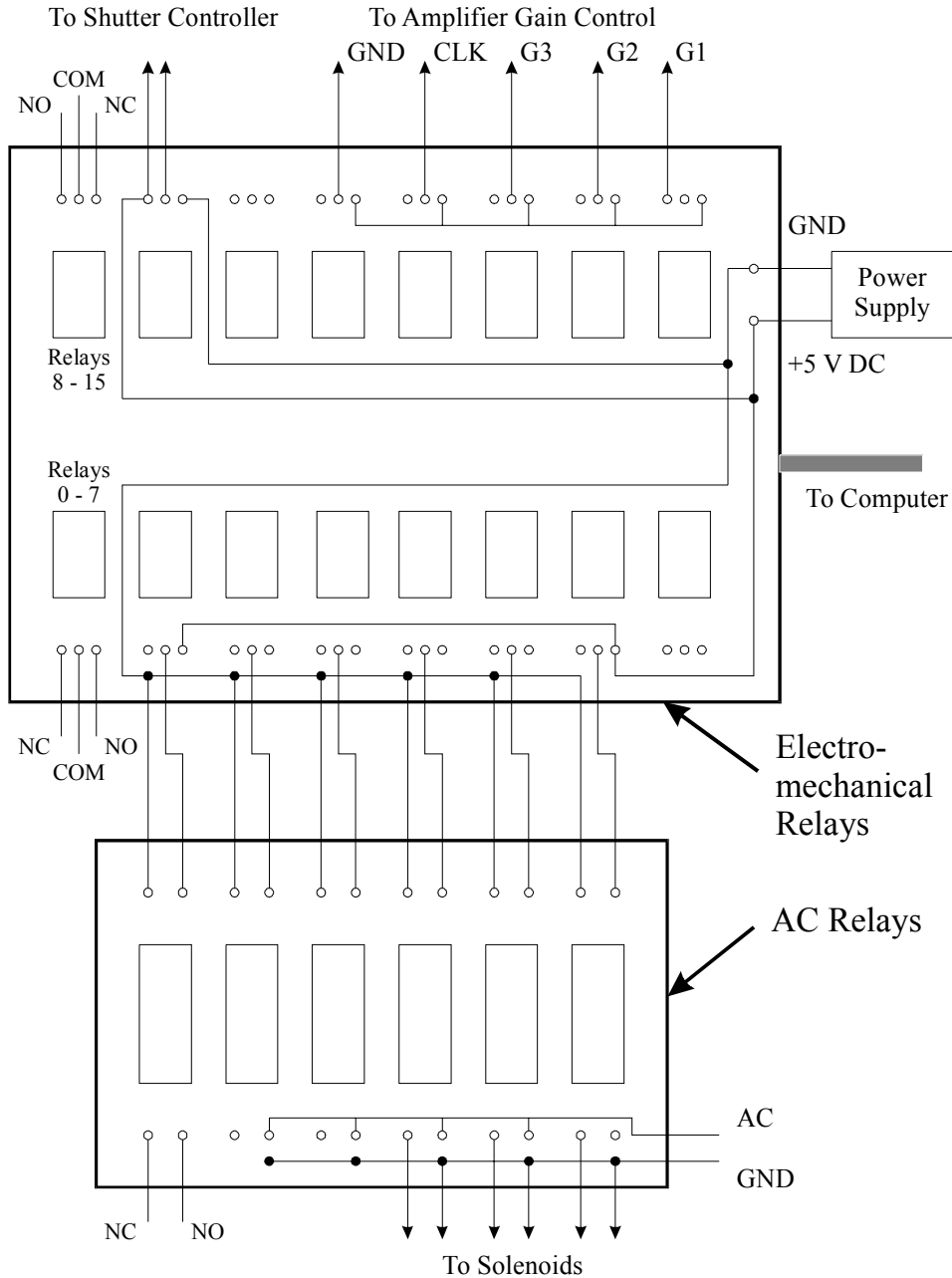


Figure 3.6 Electrical connections for the electro-mechanical relays and the AC relays.

Separate power supplies provide the dc voltages needed by the photodiode amplifier and the electro-mechanical relays, while a temperature controller maintains the photodiode at a constant temperature. A digital voltmeter measures the signal from the photodiode amplifier.

4. Characterization of Instrument

The instrument was thoroughly characterized not only to ensure proper operation but also to verify compliance with the applicable standards for measuring transmission density [2,3,4]. These standards specify both the geometrical and spectral conditions for this measurement. The characterization is detailed for the source and detector systems and for the step tablet films.

The relative spectral flux distribution of the source, denoted by S_H , is specified in [4]. This distribution depends upon the opal, infrared optical filter, and current through the lamp. With the type of opal, lamp, and filter fixed, as well as the thickness of the filter, the only adjustable parameter is the current. Therefore, the optimal current to achieve a close approximation of S_H was determined experimentally.

The relative spectral flux distribution of the source at different lamp currents was measured by a spectroradiometer in the Low-Level Radiance facility [6]. The source system was placed on its side so that the opal was imaged onto the entrance slit of the monochromator. The spectral radiant flux emerging from the exit slit of the monochromator was measured with a Si photodiode. The spectral radiance responsivity of the spectroradiometer – imaging optics, monochromator, and photodiode – was determined by measuring the signal $S_s(\lambda)$ when the output port of an integrating sphere with known radiance $L_s(\lambda)$ was imaged onto the monochromator entrance slit. The signal from the opal $S_o(\lambda)$ was then measured for different lamp currents. The radiance of the opal $L_o(\lambda)$ was calculated using

$$L_o(\lambda) = \frac{S_o(\lambda)}{S_s(\lambda)} \cdot L_s(\lambda) \quad (4.1)$$

and normalized to have a value of 100 at 560 nm to compare with S_H .

The best agreement between S_H and the measured relative spectral flux distribution was obtained with a lamp current of 7.8 A. These two distributions are shown as a function of wavelength in figure 4.1, with the distribution of the instrument denoted by S_I . This distribution was relatively insensitive to changes in lamp current of 0.1 A. For greater changes in current, the measured distribution at wavelengths less than 600 nm was either obviously greater or less than S_H for increased or decreased currents, respectively. Since the lamp power supply maintains a constant current to within 1 mA, the distribution S_I is not expected to change during measurements of step tablet films.

The spectral reflectance $\rho_o(\lambda)$ is specified to be 0.55 ± 0.05 [4]. The 6° - hemispherical reflectance of flash opals of the same type used in the instrument was

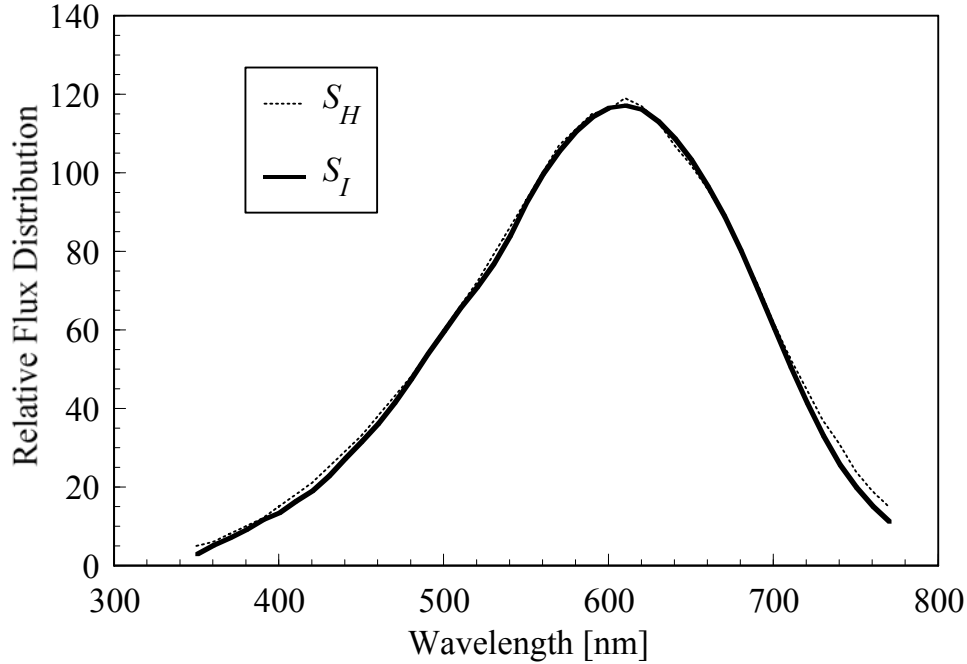


Figure 4.1 Relative flux distribution specified by the standards, S_H , and achieved by the instrument at a lamp current of 7.8 A, S_I , as a function of wavelength.

measured in the Spectral Tri-function Automated Reference Reflectometer facility [7]. A flash opal with a diameter of 6 mm was mounted in the vacuum plate of the source system, which was then placed at the sample port of the integrating sphere of the reflectometer. A converging lens reduced the monochromatic incident beam diameter to approximately 4 mm. Since this diameter was larger than the 3 mm diameter of the opal used in the instrument, a 6 mm diameter opal was measured instead. The angle of incidence of the beam on the opal was 6° , and both the specular and diffuse components of reflection were included in the integrating sphere. The radiant flux at the detector port of the integrating sphere was measured with a Si photodiode. At each wavelength of the incident beam, the signal from reflection from the opal $S_o(\lambda)$ and the signal from reflection from the integrating sphere wall $S_w(\lambda)$ were measured. Since the spectral reflectance of the wall $\rho_w(\lambda)$ is known, the spectral reflectance of the opal $\rho_o(\lambda)$ is calculated from

$$\rho_o(\lambda) = \frac{S_o(\lambda)}{S_w(\lambda)} \cdot \rho_w(\lambda) . \quad (4.2)$$

The reflectance of a flash opal as a function of wavelength is shown in figure 4.2. The reflectance of all three 6 mm diameter opals cut from the same large piece were the same, and this reflectance is expected to apply to the 3 mm diameter opal used in the instrument. The reflectance decreases monotonically with wavelength and is within the values specified by the standard for wavelengths longer than 490 nm. The effect of this

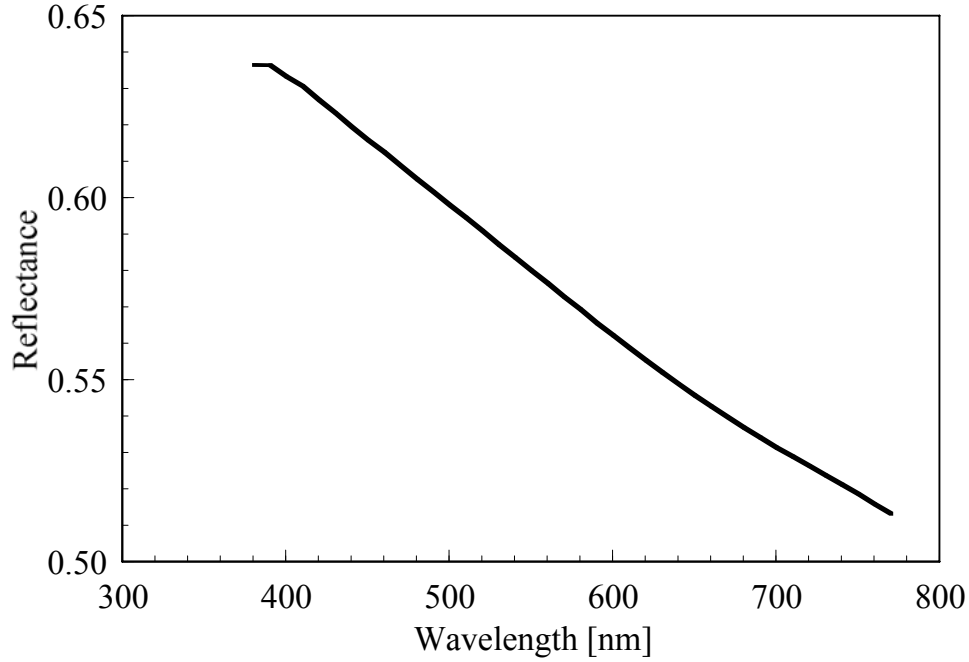


Figure 4.2 6° - hemispherical reflectance of the opal as a function of wavelength.

discrepancy between the actual opal reflectance and the standard reflectance is discussed in section 6.

The diffusion coefficient d of the opal is specified to be greater than or equal to 0.9 [4]. The radiant flux from the opal was measured as a function of polar angle θ using the bi-directional reflectance goniometer of the Spectral Tri-function Automated Reference Reflectometer facility [7]. The entire source system was placed on its side so that the opal was centered in the sample holder of the goniometer and the face of the opal was on the axis of rotation of the detector arm. The lamp was operated at a current of 7.8 A and water was circulated through the lamp housing and water filter. A green filter was placed in front of the Si photodiode on the detector arm to simulate the spectral conditions of the transmission density instrument detector system.

The signal $S(\theta)$ was measured at polar angles of the detector from -80° to $+80^\circ$ in 5° steps. The signals were normalized by the signal at 0° , $S(0)$, to yield $s(\theta)$. These normalized signals are proportional to the factor $\frac{L_j(\theta)}{L_j(0)} \cdot \cos\theta$ in eq (2.30). The

normalized signal, divided by $\cos\theta$, as a function of polar angle is shown in figure 4.3. For an ideal, Lambertian diffuser, this ratio is one at all angles. The decrease of this ratio as the angle increases indicates that the opal is not an ideal diffuser. There are two methods for calculating the diffusion coefficient. The first is given in [4],

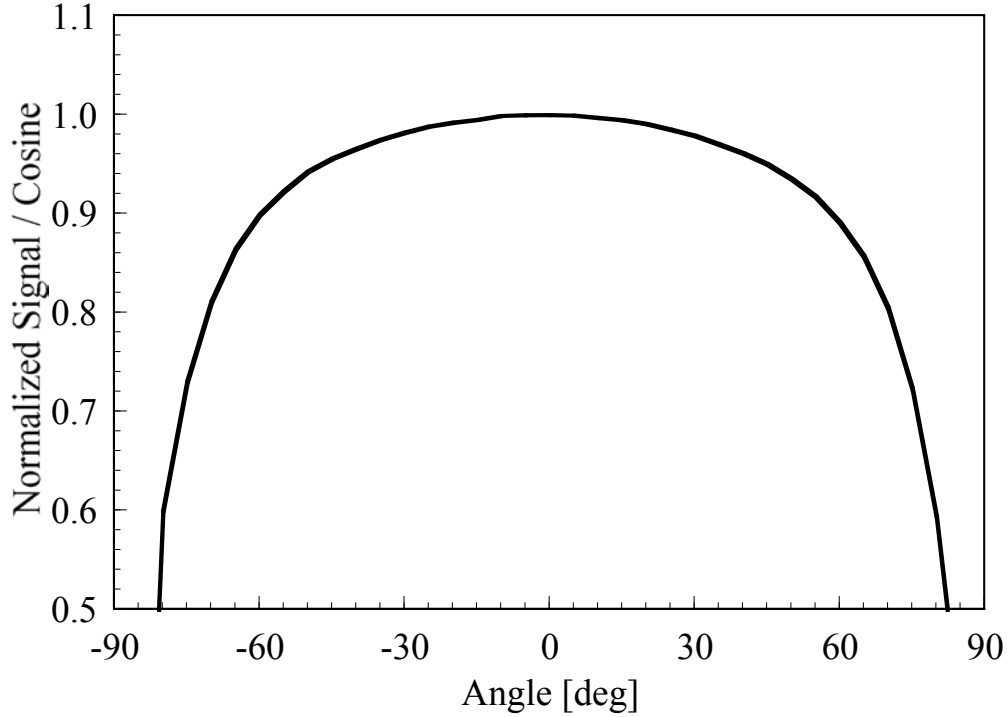


Figure 4.3 Normalized signal of the efflux from the opal divided by the cosing of the angle as a function of angle.

$$d = \frac{\sum s(\theta)}{\sum \cos \theta} , \quad (4.3)$$

where the summation is over all the angles at which signals were measured. The second method is adapted from eq (2.30), which was originally derived in [5], and is given by

$$d = \frac{\sum s(\theta) \cdot \sin \theta}{\sum \cos \theta \cdot \sin \theta} . \quad (4.4)$$

The diffusion coefficient calculated using eq (4.3) is $d = 0.95$, while using eq (4.4) $d = 0.91$. Both of these values are greater than 0.90.

The spectral response of the detector system V_T is specified in [4] and is given by eq (2.3), namely

$$S_A \cdot V_\lambda = S_H \cdot V_T . \quad (4.5)$$

Here, S_A is the relative spectral flux distribution of Illuminant A, V_λ is the photopic spectral luminous efficiency function, and S_H is the relative spectral flux distribution specified in [4]. The spectral response of the detector system is the product of the

specified spectral response V_T . There is an obvious discrepancy between the two spectral responses for wavelengths longer than 570 nm. However, V_I closely approximates V_λ , which is expected since the filter was designed so that the spectral response obtained in combination with the Si photodiode is V_λ . Because the photopic spectral luminous efficiency function is widely used, and because no filter could be readily found to modify V_I to V_T , no attempt was made to obtain V_T . The effect of the discrepancy between V_T and V_I is discussed in section 6.

To use eq (2.22) to calculate transmission density from the signals and gains, the linearity of the photodiode and the ratio of gains G_τ / G_j must be determined accurately. The linearity of the photodiode-amplifier combination was measured in the Beamconjoiner facility [10]. This facility uses the beam addition method with sets of filters on each beam path to automatically vary the radiant flux on the detector by three decades. The source system of the transmission density instrument provided the input flux. The linearity was determined at each gain setting of the amplifier, the maximum radiant flux incident on the detector being controlled by the lamp current and neutral-density filters in front of the photodiode. The relative responsivity, defined as the ratio of the measured signal to the incident radiant flux as a function of current from the photodiode is shown in figure 4.5 at several gain settings. A relative responsivity of one corresponds to ideal linearity. The relative responsivity of the photodiode - amplifier combination is very close to one for gain settings 5 to 8. Deviations from one occur at gain setting 9, mostly due to the small currents at this gain setting.

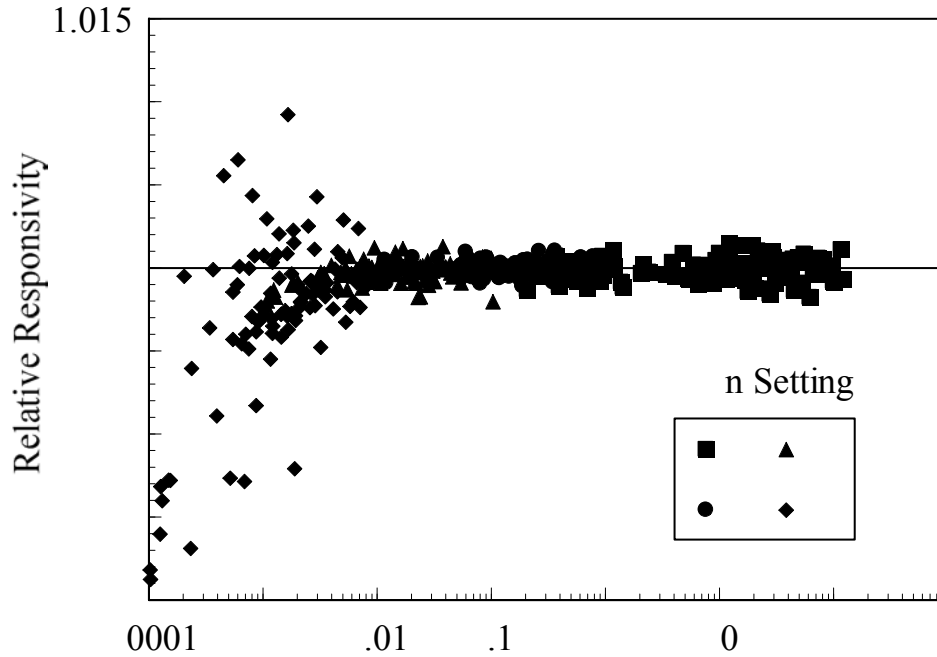


Figure 4.5 Relative responsivity (measured signal divided by actual flux) of the photodiode and amplifier as a function of current at the indicated gain settings.

... and the grain size photographic film step across. There is spectral structure in these properties for the x-ray film, giving it a blue tint, while the neutral photographic film has no such spectral structure.

Table 4.1 Values of successive gain ratios

Gain Ratio	Value	Relative Standard Uncertainty
G_5 / G_4	10.00032	4.13×10^{-6}
G_6 / G_5	10.00493	6.31×10^{-5}
G_7 / G_6	10.00311	4.62×10^{-5}
G_8 / G_7	10.00098	5.29×10^{-5}
G_9 / G_8	9.97574	1.09×10^{-5}
G_{10} / G_9	10.01515	2.36×10^{-4}

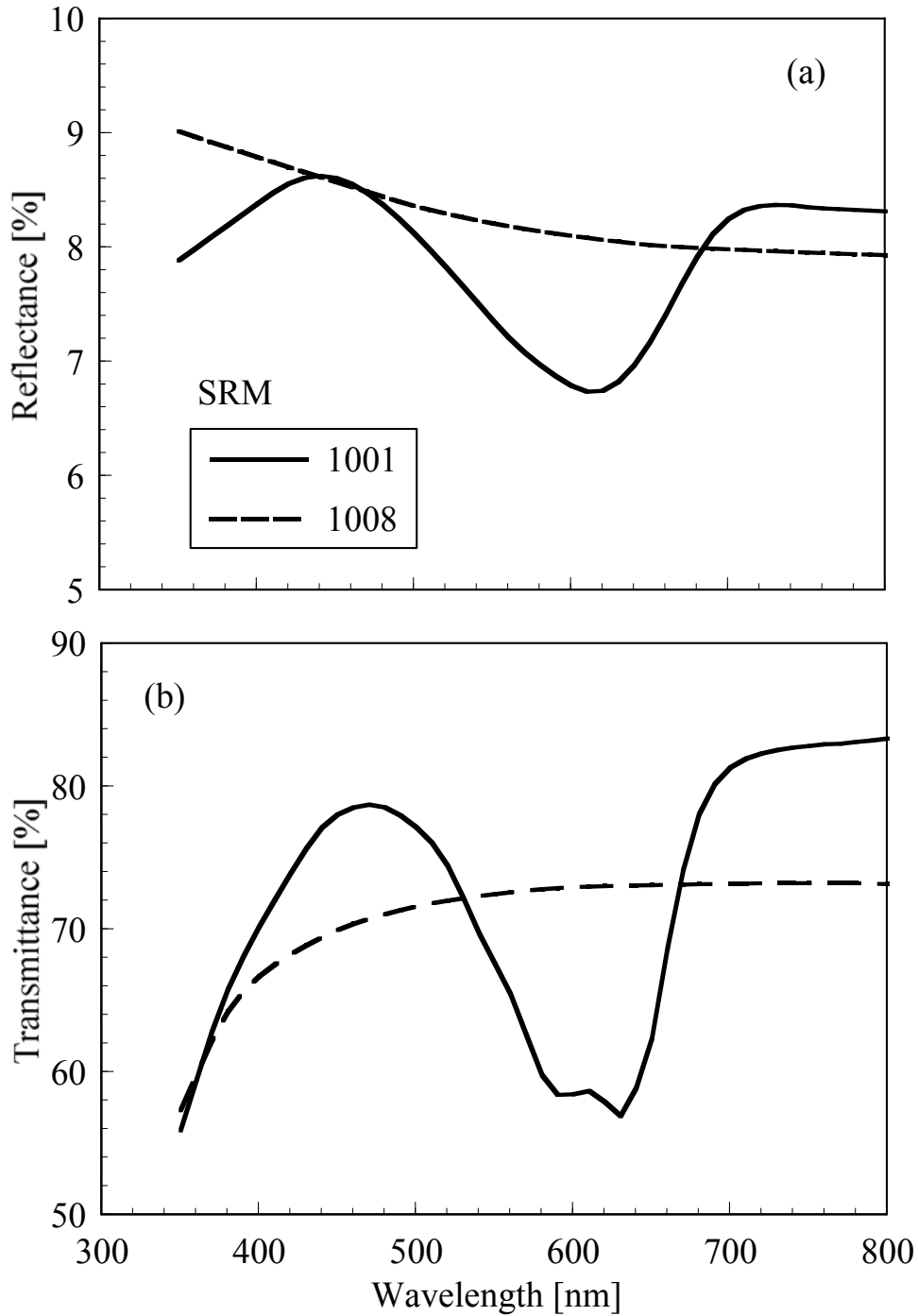


Figure 4.6 Reflectance and transmittance of the indicated films as a function of wavelength.

Several other geometrical conditions are specified by [3] in addition to the diffusion coefficient of the opal. The half-angle of the acceptance cone must be less than 10° . From the description of the lens system in the previous section, the half-angle of the

instrument is 9.5° . The film must be in contact with the opal when the efflux is measured, which is achieved by pulling the film onto the opal with a vacuum.

The transmission density is to be measured at the center of each step. Centering the steps on the opal is accomplished by optical means in the transverse direction of the steps and by mechanical means in the longitudinal direction. Note that the transverse direction of a step corresponds to the longitudinal direction of the film step tablet. The step widths are equal for each type of film and the position along the longitudinal direction of the film is continuously adjustable with the horizontal translation stage. Therefore, all that is required to center the opal in the transverse direction of each step is to determine the location of a reference position on each film. This is done by measuring the signal from the opal as the film is moved in the longitudinal direction in increments of 0.08 mm from the first to the second step. The signal decreases at the boundary between the steps; the location at which the signal has decreased by 5 % from its value in the first step is the reference position. Knowing this position sets the locations of the centers of each step along their transverse direction. The center along the longitudinal direction is set mechanically. The positions of the horizontal translation stage and the film holder are adjusted so that the film holder is centered on the opal over its entire length. This fixes the positions of the stage and holder. The posts on the film tray are then adjusted to give the minimum possible clearance between them and the film holder. This centers the films in the tray and thereby the longitudinal direction of the steps.

The instrument was designed to measure diffuse visual transmission density according to spectral and geometrical conditions specified by the applicable standards. The conditions are satisfied by the instrument, with the exception of the opal reflectance and the spectral response. The effects of these discrepancies between the standards and the instrument are detailed in section 6.

5. Operation of Instrument

The instrument automatically measures the transmission density of each step of a batch of step tablet films. The setup for the measurements is fairly simple. The films are loaded into the film holder in the order in which they are to be measured, with the serial numbers face-down so that the correct side of the film will be in contact with the opal. The serial numbers of the films are entered in a separate text file, which is used by the program during the measurements to keep track of the films. The digital voltmeter is setup to auto-zero and to use ten power line cycles for each reading. The lamp is operated at 7.8 A for a thirty minute warm-up period, the room lights are turned off, and the measurements are begun.

For each film, the film holder is moved horizontally over the film tray and then vertically until the holder is in contact with a film. The vertical spring-loaded stage allows the film holder to remain stationary and in contact with the film while the vertical translation stage continues to move downward, preventing unnecessary torques on the holder. The vacuum is applied, attaching the film to the holder. The signal from the aperture flux is measured at a gain setting of 5 by closing the shutter, recording five

readings from the voltmeter, opening the shutter, and recording five more readings. The signals measured with the shutter closed are referred to as dark signals. The holder is then translated vertically and horizontally until the first step of the film is 1.6 mm above the opal. The signal is measured to verify that a film is attached to the film holder; if not, the process is repeated until a film is attached. The boundary between the first and second steps is found, as described in the previous section. This sets the location of the horizontal translation stage so that the centers of the steps are measured.

To measure the signal from the transmitted flux of a step, the film is moved horizontally to center the step on the opal, the film is lowered until it is on top of the opal, and a vacuum is applied with the vacuum plate while the vacuum on the film holder is released. This pulls the film into close contact with the opal, and five readings from the voltmeter are recorded. A vacuum is applied to the film holder while it is released from the vacuum plate, which attaches the film to the holder. The holder is then raised and the process is repeated for the next step. If the signal from a step is less than 1.3 V, the gain setting for the next step is increased by one and a dark signal is measured prior to measuring the signal from the transmitted flux. After the last step is measured, the film is moved over the other film tray, the vacuum on the film holder is released and air is introduced into the line, and the film falls onto the tray. The signal from the aperture flux is then measured as before.

The transmission density is calculated from the signals and ratios of the gain settings. Each set of five signal readings are averaged, and the dark signals at each gain setting are subtracted from those signals obtained at that setting to yield the net signals. The two net signals for the aperture flux are averaged to yield the final aperture signal S_j . For each step, the transmission density is calculated using eq (2.22),

$$D_T = \log_{10} \left(\frac{S_j}{S_\tau} \cdot \frac{G_\tau}{G_j} \right), \quad (5.1)$$

where S_τ is the net signal from the transmitted flux at each step and G_τ / G_j is the gain ratio. The signal from the aperture flux is approximately 1.5 V on gain setting 5. For $D_T = 4$, this corresponds to a signal of 1.5 V at gain setting 9. Therefore, only gain

Table 5.1 Values of the gain ratios used to calculate transmission density

Gain Ratio	Value	Relative Standard Uncertainty
G_6 / G_5	$1.000\,493 \times 10^1$	6.31×10^{-5}
G_7 / G_5	$1.000\,804 \times 10^2$	7.82×10^{-5}
G_8 / G_5	$1.000\,903 \times 10^3$	9.44×10^{-5}
G_9 / G_5	$0.998\,475 \times 10^4$	9.50×10^{-5}

settings 5 to 9 are used for calibrating the SRMs. The gain ratios, relative to gain setting 5, are listed in table 5.1, along with the relative standard uncertainties.

A batch of films is measured on three separate occasions in both ascending and descending serial number order. The average of the three determinations is reported on the calibration certificate as the transmission density of a step. The standard deviation of the three determinations must be less than the expanded uncertainty due to random effects, detailed in the next section. Sample calibration certificates are given in Appendices A and B. Proper operation of the instrument is verified by including in each batch several check standard films that were measured previously. These check standard films were randomly chosen from each lot of films received from the manufacturer.

6. Uncertainties

Each measurement of transmission density has an uncertainty associated with it. This section details the components of uncertainty, their evaluation, and the resulting uncertainty in transmission density. This uncertainty analysis follows the guidelines given in [11].

In general, the purpose of a measurement is to determine the value of a measurand y , which is obtained from n other quantities x_i through the functional relationship f , given by

$$y = f(x_1, x_2, \dots, x_i, \dots, x_n) . \quad (6.1)$$

The standard uncertainty of an input quantity x_i is the estimated standard deviation associated with this quantity and is denoted by $u(x_i)$. The relative standard uncertainty is given by $u(x_i) / x_i$. The standard uncertainties may be classified either by the effect of their source or by their method of evaluation. The effects are either random or systematic, the former arising from stochastic temporal or spatial variations in the measurement and the later from recognized effects on a measurement. The method of evaluation is either Type A, which is based on statistical analysis, or Type B, which is based on other means.

To first order, the estimated standard uncertainty $u(y)$ in the measurand due to a standard uncertainty $u(x_i)$ is

$$u(y) = \frac{\partial f}{\partial x_i} u(x_i) , \quad (6.2)$$

where $\partial f / \partial x_i$ is the sensitivity coefficient. The combined standard uncertainty $u_c(y)$ in the measurand is the root-sum-square of the standard uncertainties associated with each quantity x_i , assuming that these standard uncertainties are uncorrelated. The expanded uncertainty U is given by $k \cdot u_c(y)$, where k is the coverage factor and is chosen on the basis of the desired level of confidence to be associated with the interval defined by U . For these SRMs, $k = 3$, which defines an interval having a level of confidence of

approximately 99.73 %. While a coverage factor $k = 2$ is customary for the expanded uncertainty [11], the larger coverage factor maintains consistency with previous SRMs of these types and is accepted by users because of the use of the SRMs in the areas of health and safety.

The components of uncertainty for transmission density are conveniently divided into those arising from the signal measurements, the uniformity of each step, and agreement with the appropriate standards [3,4]. In the first case, the appropriate measurement equation is eq (2.22), while for the last case eqs (2.23) and (2.31) are applicable. Expressing eq (2.22) as

$$D_T = \log_{10}(x) \quad (6.3)$$

where x can be a signal or the gain ratio, the sensitivity coefficient is

$$\frac{\partial D_T}{\partial x} = 0.434 \cdot \frac{1}{x} . \quad (6.4)$$

Therefore, the standard uncertainty $u(D_T)$ due to the standard uncertainty $u(x)$ is

$$u(D_T) = 0.434 \cdot \frac{u(x)}{x} . \quad (6.5)$$

Note that the standard uncertainty of D_T is proportional to the relative standard uncertainty of x .

There are several components of uncertainty associated with calculating transmission density from eq (2.22), which assumes that the signals are directly proportional to the fluxes. In addition, the same influx is assumed when measuring S_j and S_τ . These components are the accuracy of the digital voltmeter, signal noise, lamp stability, detector linearity, and the gain ratio.

The uncertainty arising from the accuracy of the digital voltmeter is a systematic effect with a Type B evaluation and assuming a normal probability distribution. Using the manufacturer's specifications, the relative standard uncertainty of S_j is 23×10^{-6} , while the maximum relative standard uncertainty of S_τ is 77×10^{-6} . The combined relative standard uncertainty of S_j / S_τ is therefore 80×10^{-6} which, using eq (6.5), results in a standard uncertainty $u(D_T) \ll 0.001$.

Signal noise and lamp stability result in uncertainties from random effects with Type A evaluations. A typical relative standard deviation of the signal calculated from measurements of ten different films is 0.002, which results in a standard uncertainty $u(D_T) = 0.001$. Likewise, a typical relative standard deviation of the signal from the aperture flux monitored over a period of 15 min is 0.002.

The uncertainties arising from the detector linearity and the gain ratio are systematic effects with Type A evaluations. The signals are always between 0.1 V and 12 V at each gain setting, except for gain setting 9, for which the minimum signal is 1 V. The maximum relative standard deviation of the relative responsivity of the photodiode - amplifier combination, subject to the ranges of the signals, is 0.0028, resulting in a standard uncertainty $u(D_T) = 0.001$. The relative standard uncertainties for the gain ratios are given in table 5.1, resulting in a standard uncertainty $u(D_T) < 0.001$.

The transmission density is supposed to be determined at the center of each step. However, if the transmission density of a step is not uniform, an uncertainty in centering the opal results in an uncertainty in the measured transmission density. The standard uncertainty in centering the opal along the transverse direction of a step depends upon finding the boundary between the first and second steps of a film and knowing the spacing between the centers of the steps, and is 0.5 mm. The standard uncertainty for the longitudinal direction depends upon the mechanical adjustments of the film holder and the posts on the film tray so that the transverse direction of the film is centered on the opal along the entire length of the film. The standard uncertainty in centering in this dimension is 1 mm.

The uniformity of the transmission densities of the steps of five representative films of each type of SRM was determined by measuring the transmission density every 0.17 mm along three lines running the length of each film. One line was centered along the width of the films, the other two were displaced by -1.5 mm and $+1.5$ mm from the center line. All the transmission densities varied by much less than 0.001 within 0.5 mm of the center in the transverse direction of the steps and by approximately 0.001 within 1 mm of the center in the longitudinal direction. Therefore, the standard uncertainty $u(D_T)$ due to the uniformity of the steps is 0.001.

As mentioned in section 4, neither the opal reflectance nor the spectral product are in agreement with the standards specified in [4]. The uncertainties arising from these two components are systematic effects evaluated using Type B methods and a normal probability distribution. The standard uncertainties are estimated from eq (2.23) using the measured transmittance $\tau_s(\lambda)$ and reflectance $\rho_s(\lambda)$ of the films and separating the effects of the two components by assuming either an ideal spectral product or opal reflectance.

The diffusion coefficient $d = 0.91$ is within the range of values specified in [3]. Therefore, the standard uncertainty arising from this component is less than 0.001. However, instruments using opals with different diffusion coefficients could measure significantly different transmission densities. Using eq (2.31), the difference in transmission density ΔD_T due to different diffusion coefficients is

$$\Delta D_T = \log_{10} \left(\frac{d_o}{d} \right), \quad (6.6)$$

where d_o is the diffusion coefficient of the opal used in this instrument and d is the diffusion coefficient of another instrument. From [3], the minimum acceptable value of d is 0.9, while from [5] the physically maximum value is 0.95. Therefore, from eq (6.6) ΔD_T can range from +0.005 to -0.019.

As shown in figure 4.2, the opal reflectance $\rho_o(\lambda)$ is greater than the acceptable maximum of 0.6 [4] for wavelengths shorter than 490 nm. The standard uncertainty $u(D_T)$ is estimated from eq (2.23) by calculating D_T for different values of $\rho_o(\lambda)$ using

$$D_T = \log_{10} \left(\frac{\int S_H(\lambda) \cdot V_T(\lambda) \cdot d\lambda}{\int S_H(\lambda) \cdot \frac{\tau_s(\lambda)}{1 - \rho_o(\lambda) \cdot \rho_s(\lambda)} \cdot V_T(\lambda) \cdot d\lambda} \right). \quad (6.7)$$

Values of D_T for different opal reflectances and both types of films are given in table 6.1. Since the transmission densities calculated using the actual opal reflectance are within the ranges obtained from the acceptable opal reflectances, the standard uncertainty $u(D_T)$ associated with the opal reflectance is less than 0.001.

Table 6.1 Calculated values of transmission density for both types of step tablet films at various opal reflectances

Opal Reflectance	Step Tablet Film	
	X-Ray (SRM 1001)	Photographic (SRM 1008)
0.50	0.173	0.121
0.55	0.172	0.118
0.60	0.171	0.117
actual	0.171	0.118

Finally, the spectral product of the instrument $S_I \cdot V_I$ is not $S_H \cdot V_T$, but approximately $S_H \cdot V_\lambda$ since the spectral response of the detector is nearly the photopic spectral luminous efficiency function. The standard uncertainty $u(D_T)$ is estimated from eq (2.33) by calculating the transmission densities obtained with the ideal and actual spectral products, using the ideal opal reflectance $\rho_o(\lambda) = 0.55$. The difference in transmission density ΔD_T is given by

$$\Delta D_T = \log_{10} \left(\frac{\int S_I(\lambda) \cdot V_I(\lambda) \cdot d\lambda}{\int S_I(\lambda) \cdot \frac{\tau_s(\lambda)}{1 - 0.55 \cdot \rho_s(\lambda)} \cdot V_I(\lambda) \cdot d\lambda} \right) - \log_{10} \left(\frac{\int S_H(\lambda) \cdot V_T(\lambda) \cdot d\lambda}{\int S_H(\lambda) \cdot \frac{\tau_s(\lambda)}{1 - 0.55 \cdot \rho_s(\lambda)} \cdot V_T(\lambda) \cdot d\lambda} \right) \quad (6.8)$$

Using eq (6.8), $\Delta D_T = 0.000\ 282$ and $0.000\ 002$ for the x-ray and photographic films, respectively. This results in a standard uncertainty $u(D_T) < 0.001$ for both types of films. Since the reflectance and transmittance of the photographic films are relatively constant over the wavelength range for which the spectral product is appreciable, ΔD_T is expected to be nearly zero for these films.

The standard uncertainty $u(D_T)$ resulting from each component of uncertainty is given in table 6.2, along with the combined and expanded uncertainties for each SRM. The only components that contribute to the combined uncertainty are the signal noise, lamp stability, detector linearity, and step uniformity, all of which except the detector linearity are caused by random effects. The expanded uncertainty from these random effects is 0.005. Therefore, as mentioned at the end of the previous section, the standard deviation of the three determinations of the transmission densities of a step must be less than 0.005 to accept the average as the reported transmission density of the step. Otherwise, the instrument is assumed to have malfunctioned in some manner during one of the runs and the film is measured again. Note that even though the opal reflectance and the spectral product do not comply with those specified in the standards [4], the resulting standard uncertainty in transmission density is less than 0.001 in both cases.

6. Conclusions

The instrument detailed in this Special Publication measures the diffuse visual transmission density of both x-ray film (SRM 1001) and photographic film (SRM 1008) step tablets using the diffuse influx mode. It is fully automated so that many films can be measured in one batch run. Comprehensive characterizations of the instrument were performed to ensure that it complies with the relevant international standards for these measurements. The expanded uncertainty ($k = 3$) for transmission density is 0.006.

Acknowledgments

Funding for the diffuse transmission densitometer was provided by the Standard Reference Materials Program under the direction of Nancy Trahey. Design, construction, and characterization of the diffuse transmission densitometer benefited from the efforts of Daniel Dummer, Christopher Cromer, and Xiaxiong Xiong, all of the Optical Technology

Division, and from discussions with Michael Goodwin and Philip Wychorski of the Eastman Kodak Co.

Table 6.2 Components of uncertainty and the resulting standard uncertainties in transmission density

Component of Uncertainty	Effect ^{a)}	Type ^{b)}	Standard Uncertainty $u(D_T)$
Voltmeter Accuracy	S	B	$\ll 0.001$
Signal Noise	R	A	0.001
Lamp Stability	R	A	0.001
Detector Linearity	S	A	0.001
Gain Ratio	S	A	$\ll 0.001$
Step Uniformity			
X-Ray Film	R	A	0.001
Photographic Film	R	A	0.001
Diffusion Coefficient	S	B	< 0.001
Opal Reflectance			
X-Ray Film	S	B	< 0.001
Photographic Film	S	B	< 0.001
Spectral Product			
X-Ray Film	S	B	< 0.001
Photographic Film	S	B	$\ll 0.001$
Combined Uncertainty $u_c(D_T)$			
X-Ray Film (SRM 1001)			0.002
Photographic Film (SRM 1008)			0.002
Expanded Uncertainty $U (k = 3)$			
X-Ray Film (SRM 1001)			0.006
Photographic Film (SRM 1008)			0.006

^{a)} R = random, S = systematic

^{b)} A = Type A evaluation, B = Type B evaluation

References

- [1] C. S. McCamy, "Concepts, Terminology, and Notation for Optical Modulation," *Photogr. Sci. Eng.* **10**, 314 (1966).
- [2] ISO 5-1: Photography – Density Measurements – Part 1: Terms, Symbols, and Notations (1984).
- [3] ISO 5-2: Photography – Density Measurements – Part 2: Geometric Conditions for Transmission Density (1991).
- [4] ISO 5-3: Photography – Density Measurements – Part 3: Spectral Conditions (1984).
- [5] E. Buhr, D. Hoeshen, and D. Bergmann, "The Measurement of Diffuse Optical Densities. Part I: The Diffusion Coefficient," *J. Imag. Sci. and Technol.* **39**, 453 (1995).
- [6] James H. Walker and Ambler Thompson, "Spectral Radiance of a Large-Area Integrating Sphere Source," *J. Res. Natl. Inst. Stand. Technol.* **100**, 37 (1995).
- [7] P. Yvonne Barnes, Edward A. Early, and Albert C. Parr, "NIST Measurement Services: Spectral Reflectance," *Natl. Inst. Stand. Technol., Spec. Publ. 250-48* (1998).
- [8] Thomas C. Larason, Sally S. Bruce, and Albert C. Parr, "NIST Measurement Services: Spectroradiometric Detector Measurements: Parts I and II - Ultraviolet and Visible to Near Infrared Detectors," *Natl. Inst. Stand. Technol., Spec. Publ. 250-41* (1997).
- [9] Kenneth L. Eckerle, Jack J. Hsia, Klaus D. Mielenz, and Victor R. Weidner, "Regular Spectral Transmittance," *Natl. Bur. Stand. (U.S.), Spec. Publ. 250-6* (1986).
- [10] Ambler Thompson and How-More Chen, "Beamcon III, a Linearity Measurement Instrument for Optical Detectors," *J. Res. Natl. Inst. Stand. Technol.* **99**, 751 (1994).
- [11] Barry N. Taylor and Chris E. Kuyatt, "Guidelines for Evaluating and Expressing the Uncertainty of NIST Measurement Results," *Natl. Inst. Stand. Technol. Tech. Note 1297* (1994).